Accepted Manuscript

Cold spray deposition of a Ni-WC composite coating and its dry sliding wear behavior

S.A. Alidokht, P. Manimunda, P. Vo, S. Yue, R. R. Chromik

Cold spray deposition of a Ni-WC composite coating and its dry sliding wear behavior

S.A. Alidokht [a], P. Manimunda [a], P. Vo [b], S. Yue [a], R. R. Chromik [a]

[a] Department of Mining and Materials Engineering, McGill University, M.H.Wong Building, 3610 University Street, Montreal, QC H3A 0C5, Canada

[b] National Research Council Canada, 75, boul. de Mortagne, Boucherville, QC J4B 6Y4, Canada

Abstract

Ni-WC composite are ideal protective coatings against wear that are often fabricated using laser cladding. However, high temperature of laser cladding and associated materials melting may result in non-homogenous distribution of WC particles, as well as decarburization and considerable residual stress and a deterioration of the wear resistance. An alternative is to use cold spray to deposit WC based composite coatings. The lower temperature allows one to retain the composition of initial WC feedstock but the cold spray process is only recently being researched for development of composite coatings. In this study, Ni and Ni-WC coatings were fabricated by cold spray. The WC and Ni powders were fed to a de Laval nozzle from separate hoppers with independent feed rates. By adjusting feedrates, a blend of Ni-36.2vol% WC was sprayed, which resulted in a composite coating of Ni-10.5vol.% WC. The influence of WC on Ni deposition was examined via microstructural characterization, including morphology of the coating's top surface and polished cross sections. Mechanical properties of coatings were improved by incorporation of WC into the Ni matrix. The wear behavior of coatings was studied with reciprocating sliding wear tests using a 6.35 mm diameter WC-Co ball. All tests were conducted in dry air with a sliding speed of 3 mm/sec, a track length of 10 mm, and normal load of 5 N. WC-Ni coatings were more wear resistant than cold-sprayed Ni coatings. The correlations

between worn surface morphologies, subsurface microstructure induced by wear and the wear behavior of the coatings was discussed. Microstructural analyses showed a mechanically mixed layer (MML) on the top of worn surfaces consisting of compacted oxides. It was revealed that the presence of hard particles in the Ni-WC coating facilitated fast development of the MML, as well as stabilized the MML, characterized by less plastic flow, fewer cracking and higher hardness.

Keywords: Cold spray, Metal matrix composite, Friction, Mechanically mixed layer (MML), WC, Subsurface microstructure

1. Introduction

Metal matrix composites (MMCs) have long been used to enhance the wear resistance in demanding engineering applications [1]. One such system is Ni and Ni-based alloys, which exhibit high toughness and corrosion resistances that are reinforced using hard secondary phases to improve their tribological properties [2]. MMCs of WC in metal matrices, including Ni, are widespread due to a good combination of hardness and toughness, and improved wear resistance [3,4]. One of the widely used methods for obtaining these composite coatings is laser cladding, which allows melting of high temperature materials. Previous studies have reported very good adhesion of laser cladded MMCs to the substrate as well as low porosity [3-7]. However, a non-homogenous distribution of WC particles was reported. Due to higher density of WC reinforcement particles compared to molten Ni, they tend to precipitate and concentrate at the bottom of the coating [3-5]. This causes non- homogenous distribution of WC particles, whereas for wear resistance application, a high concentration of WC at the top surface is needed. Moreover, in order to obtain thicker coatings and higher concentration of hard phase inside matrix, the larger laser power is needed, which can result in unwanted chemical changes and

significant residual stress [3-7]. Specifically for WC containing systems, the high temperature during laser cladding causes dissolution of carbide by melted binder phase, thermal dissociation of WC, and loss of carbon [5-7]. The result is that brittle phases, such as W_2C, W and/or Ni_2W_4C intermetallic phases are present in the coating, especially at the interfaces. While the process can be optimized to minimize these effects, presence of these defects increases the wear rate, primarily due to cracking along the preferential crack paths provided by brittle phases and residual stress [3,4]. Cold spray is a solid state thermal spray process where particles are accelerated in a de Laval nozzle to supersonic velocities (500–1200 m/s) in a gas stream and impact onto a substrate. Particles remain in solid state due to quite short contact time with the high temperature gas. Besides, the gas temperature is often much lower than the melting points of the particles. Hence, high-temperature-induced decomposition of carbides and/or other phase transformations that could be detrimental for tribological performance can be avoided [8,9]. [8,9]. Furthermore, impact induced high strains and the heat generated in this process may cause partial or complete recrystallization and evolution of ultra-fine microstructure [8-10]. Continuous high velocity impact of particles may produce a shot-peening or 'tamping' effect, which results in densification and deposition of coating with nearly theoretical density [11]. This makes cold spray a promising replacement of traditional thermal spray when spraying heat sensitive materials.

Several researchers have deposited composite coatings containing WC by cold spray [12-17]. However, in most cases, pretreatment powder processing such as cladding [12] and sintering [13-16] were utilized to overcome difficulties regarding retention of hard WC particles within coating. Wang et al. [12] used electroplating and chemical vapor deposition (CVD) to deposit a Cu and Al metallic layer on WC particles. The addition of soft metal around WC particles is reported to provide necessary ductility and make particles behave like a regular soft metal

3

powder during cold spraying. Their investigation showed that coatings deposited using pre-coated carbide particles were denser, displayed higher hardness, and recovered more carbide phase compared to coatings produced from equivalent metal-carbide mixtures. More of the studies on WC containing cold sprayed coatings have used agglomerated, sintered and crushed WC-Co powders. In this regard, several approaches were employed to overcome low deposition efficiency and unsatisfactory bonding quality, which arises from non-deformability of hard phase. These strategies are including: Adequately designed porous spray powder [13-15], sufficient binder/matrix content [16], and powder preheating prior to spray [17]. Recent studies have been focused mostly on modifying feedstock powder [12-17]. This generates extra processing steps and leads to inadequate understanding of deformation and deposition mechanisms of metallic and ceramic particles upon impact during spraying. However, more investigations are needed to clarify the micro-mechanisms involved in deposition of composite coating in order to obtain desired properties.

Metallic materials, including MMCs, will develop third bodies [18] (the materials generated from first bodies) during sliding wear. As sliding progresses, detached particles from one or both surfaces are mixed to form MMLs on top of the worn surfaces [19-23]. MMLs form at the interface, and hence, separate the initial contact. Thus, tribological behavior is controlled by structural, chemical and mechanical characteristics of the MML rather than correlated only with bulk strength and hardness [21]. Gonzalez et al. [22] found that during dry sliding wear of NiCrBSi coating, the formation of a surface oxide layer, in which the rate of formation is higher than its destruction, can protect the surface below it. Studies of Jiang et al. [20] showed that oxide layers formed at 250 °C during sliding wear of a nickel-base high-temperature alloy is more wear protective, whereas at 20 °C, the real contact areas mainly consisted of loosely compacted particles. Incorporation of hard particles in metallic materials strongly affects the materials

mixing and transfer mechanisms during sliding, which in turn influences the MML efficiency to protect the first bodies from wear [23]. Fernández et al. [3] found that incorporating 7 vol% WC into a laser cladding Ni alloy enhances sliding wear resistance, by forming a continuous oxide layers and preventing adhesive wear as the main mechanism in a matrix without reinforcement particles. Meanwhile, higher concentration of WC hinders formation of MML by the collision with hard particles and the mechanical interference with the counterbody, which promotes WC fracture into small particles and leads to instability in MML. However, there is limited literature available in the field of cold-sprayed coatings' sliding wear behavior. In the present study, cold spray deposition was utilized to fabricate Ni-WC composites. The cold spray behavior of Ni and WC were studied using unmodified powders with no additional processing routes. The effect of WC on coating formation, deposition efficiency, porosity and hardness of Ni were investigated. For the two Ni and Ni-WC coatings, dry sliding wear tests were conducted and the role of WC on friction and wear was studied.

2. Experimental

Mild steel plates with thickness of 3 mm were used as substrates. Plates were cleaned in acetone and then grit blasted prior to deposition. Commercial pure water atomized Ni (Novamet, Canada) and plasma spheroidized WC (Tekna, Canada) were used as feedstock powders. Laser particle size analysis (LPSA) was used to measure feedstock powder size distribution. Cold spray was conducted using a PCS1000 system (Plasma Giken, Japan) with nitrogen as the carrier gas. Prior to entering the de Laval nozzle the gas pressure was 4 MPa and temperature was 700°C. The stand-off distance between the substrate and nozzle exit was set to 40 cm and the gun traverse speed was fixed to 30 mm/s. The particle velocities were measured in a free-jet by a time-of-flight particle diagnostic system. The WC and Ni powders were fed to the gun from separate hoppers and, by setting feed rates, a mixture of Ni-36.2vol% WC was sprayed. The co-

feeding system was used to avoid problems arising from difficulty in admixing powder of differing densities and/or damage to powders due to mechanical mixing.

Cold-sprayed coatings were cross-sectioned perpendicular to the gun traverse direction, mechanically ground, and polished to a final step by 0.05 μm colloidal silica. The morphology and microstructure of the initial powders and deposited coatings were observed by scanning electron microscopy (SEM) (FEI, Quanta 600, USA). Electron channeling contrast imaging (ECCI) using a cold field emission SEM (Hitachi, SU-8230, Japan), with photodiode BSE detector was performed to reveal the deformed structure of coatings. WC and porosity concentration within the coatings measured by image analysis by pixel count using ten random images of polished cross-sections were taken with SEM. Deposition efficiency was calculated as the weight gain divided by the mass of powder sprayed, which is the product of feed rate and the spray time. To characterize mechanical properties of initial powders and sprayed coatings, nano-hardness and macro-hardness testing were used. Nano-hardness test was performed using a Berkovich diamond tip with a triboindenter system (Hysitron, Minneapolis). The peak load, loading and unloading rate, and hold time at peak load are fixed as 5 mN, 200 μN/s and 2 s, respectively. To calculate hardness and elastic modulus, the indentation load-displacement data during indentation was analyzed using the Oliver and Pharr method [24]. Macro-hardness testing was performed using a Vickers diamond indenter. The load and holding time were 49 N and 15 s, respectively. In order to obtain an average hardness value of the composite, a large load on macro-hardness tester was used. With 49 N, the diagonal of indent was 150-160 micron and many WC particles were encountered with indents.

Sliding wear tests on the coatings were performed in dry air (0 % relative humidity) using a custom built ball on flat reciprocating tribometer. Prior to wear test, coatings were polished to a final step by 0.05 μm colloidal silica. Spheres of WC-Co with a diameter of 6.25 mm were used

as counterfaces. All tests were also conducted with normal load of 5 N, sliding speed of 3 mm/sec, and track length of 10 mm. Wear tests were run to 10, 50, 100, 500, and 1000 cycles. Friction forces were measured with a sampling rate of 800 Hz using a piezoelectric sensor mounted underneath the sample stage. Along each cycles, CoF was averaged across a central portion of the track and then graphed versus number of cycles. Worn samples were examined using a non-contact optical profilometer (Veeco instruments, USA) to obtain profiles of the wear tracks. The volume of material removed, v, was measured by multiplying the cross sectional area of material removed, measured by profilometry, by the track length. Cross-sectional area was determined by integrating height profiles across the wear track above and below the original surface, where a total number of 50 - 60 surface profile measurements per wear track were used. This, along with the total sliding distance x and applied load W, was then used to calculate wear rate (mm^3 /N m) using the equation (1) [25],

$$\acute{k} = \frac{v}{Wx} \tag{1}$$

In order to reveal wear mechanisms, worn surfaces and cross sections of wear tracks were examined using an SEM (Hitachi, SU-8230, Japan) equipped with energy dispersive X-ray spectroscopy (EDS). Nano-indentation was performed on worn surfaces to measure mechanical properties of third-bodies.

3. Results and Discussion

3.1 Powder characterization

Commercial pure Ni powders exhibited spherical morphologies and had an average powder particle size of 7 μm (Fig. 1a), which was confirmed by laser particle size analysis (Fig.1b). Grain structure of cross sectioned Ni powders revealed relatively large grain size of 1 to 10 μm (not shown here). WC particles with spherical morphologies and an approximate average

7

powder particle size of 30 µm were used as reinforcing particles in Ni-WC coatings (see Fig. 1c and d).

3.2. Coating deposition and characterization

Table 1 summarizes coatings' deposition efficiencies and thicknesses, WC in initial feedstock and in the coating, and porosity and macro-hardness of coatings. A thick and relatively dense Ni coating with 1.4 ± 0.3 mm thickness and porosity of 3.8% was deposited by cold spray (see Fig.2). Deposition efficiency was 55%. Ni particles have been accelerated to an average velocity of 650 ± 125 m/sec. Velocities of particles in the gas stream vary inversely with the square root of particles diameter, and thus, finer particles attain higher impact velocities [9]. According to Schmidt et al. [26], critical velocity can be calculated for various materials by correlating the deposition efficiencies with particle impact velocities. Critical velocity for successful deposition of Ni was calculated to be 620-680 m/s for 25 µm powder size [26]. Average powder velocity in the present study fell into this range. However, materials deformation and heat transfer analysis implies that particle size plays an important role in critical velocity. The critical velocity is higher for smaller size particles due to these effects: (1) Occurrence of shear instability in smaller particles can be hindered because of higher cooling rate and intensified strain-rate hardening, (2) Smaller size particle usually contains higher amounts of surface contaminations such as oxide shells which can have negative effect on bonding, and (3) Smaller size particles may exhibit intrinsically higher strength since they are exposed to higher quench rates during powder production [26]. In order to obtain higher deposition efficiency, higher velocities of powder are required. This can be achieved through increasing gas temperature, which not only increase particle velocity, but also decrease critical velocity by improving deformability [27]. However, due to the fact that high gas temperatures can cause nozzle clogging with Ni particles, there are technical limitations to spray Ni powder [28]. Figure

2c and d represent top surface of a cold-sprayed Ni coating. Mechanically trapped particles as well as well-deformed and highly flattened particles were observed.

Table 1- Characteristics of tested coatings.

Sample designation	DE (%)	Thickness (mm)	Porosity (%)	Macro-hardness (HV)	WC in initial feedstock (vol%)	WC in deposited coatings (vol%)
Ni	55 ± 3	1.40 ± 0.03	3.8%	368± 8	-	-
Ni-WC	22 ± 4	1.01 ± 0.01	1.1%	378± 18	36.2	10.5 ± 0.4

Figure 3 shows micrographs of a cross sectioned Ni-WC composite coating. The particles in bright contrast correspond to carbide particles and regions in dark contrast correspond to porosities. With 36.2vol% WC in initial feedstock, only around 28% of WC particles were recovered in the coating and it yielded a WC content of 10.5vol%. Low deposition efficiency and WC retention was achieved using the WC and Ni powders under the sprayed condition. More investigation is needed to explore the effect of various powders characteristics and spray parameters in order to optimize deposition condition. However, even with low deposition rate, it is believed that cold spray can be used to repair and restore a wide range of damaged components and result in life cycle improvement and major cost savings [29,30].

As can be seen from the top-view image of the sprayed composite shown in Fig. 3c and d, adding WC particles into feedstock, the top-surface of the coating was greatly altered compared to Figure 2. Interfaces between individual Ni particles were not easily visible due to improved adhesion by the tamping effect, where most of the WC particles bounced back after impacting the surface, leaving behind empty craters. A few particles penetrated deeply to the surface (see Fig. 3d). The ratio of adhered embedded particle to empty craters was significantly lower than actual

9

ACCEPTED MANUSCRIPT

WC concentration recovered to coating (measured from polished cross-sections). This was probably because of high hardness of Ni and low velocity of dense and relatively large size WC particles [31]. Therefore, during Ni-WC composite coating build up, WC particles were mainly entrapped to the coating by later-arriving Ni and WC particles, in which Ni particles deformed and surrounded WC particles [32]. There was also a large number of fine fragmented WC particles which can be observed on the top surface at some regions (Fig. 3e). As can be seen in a higher magnification view of the cross section (Fig. 3b), some of the WC particles were cracked or fragmented upon impact.

The deposition efficiency of Ni-WC was 20%. Low DE in cold sprayed MMCs is often due to low retention of the hard phase, WC in this case. A reduction in deposition efficiency of Ni was also indicated by the fact that the feed rate of Ni particles was kept same in both Ni and Ni-WC coatings, yet WC added to Ni led to a thickness reduction. This can be due to WC fragments which avoid close contact and bonding between Ni splats.

Lower porosity of cold-sprayed Ni-WC composite coating compared to Ni coating (1.1% vs 3.8%) was due to continuous high velocity impact of dense WC particles, which produced the tamping effect, and results in densification of deposited coating [11]. Macro-hardness tests were done on top surface of cold-sprayed Ni and Ni-WC coatings and the results were reported in Table 1. Macro-hardness results were inhomogeneous which is due to a non-uniform microstructure. Relatively uniform dispersion of the WC particles, which have an extremely high hardness, and densification due to tamping effect of impacting dense WC particles are the possible contributions to the higher hardness in the Ni-WC composite coating (see Table 1). However, hardness improvement due to incorporation of WC particles into Ni matrix is not significant, probably due to decreased bonding between Ni particles and fragmented/cracked WC particles.

3.3. Coatings sliding wear behavior

3.3.1. Friction and Wear

The coefficient of friction (CoF) was plotted vs number of cycles for Ni and Ni-WC coatings in Fig. 4. The two friction plots showed that Ni and Ni-WC coatings exhibited similar behavior; COF curves increased rapidly and reached steady state. The initial spike in CoF at the beginning of the sliding (see inset in Fig. 4) was linked to a localized adhering of two surfaces in contact as reported in previous studies [33]. The rupture of the adhered asperities and occupying the mating surface led to a steady value of CoF [33]. The Ni-WC coating showed a very short run-in period followed by steady state friction coefficient value of 0.71. CoF curve for Ni coating reached steady state at longer distance (150-200 cycles) and its steady state value was 0.70.

The wear rates at the end of the 10, 50, 100, 500, and 1000 cycles' tests were calculated using Eq. 1 and plotted as a function of cycle number in Fig. 5. The wear rate for both coatings was high during the initial cycles, due to adhesive wear, after which it decreased. A slight improvement in wear rate at 10 cycles for the Ni-WC composite coating may be due to decreased porosity compared to the Ni coating and load bearing effect of WC particles which reinforce materials against plastic deformation. While the wear rate of composite approached a steady state at 50 cycles, the curve of the Ni coating appeared to increase again after an initial decrease at 50 cycles. A close comparison of the graphs in Fig. 5 revealed that except for initial cycles of tests, which displayed similar wear rates for both coatings, wear rate of the composite coating was approximately seven times lower as compared to the Ni coating.

3.3.2. Worn surfaces morphologies

SEM micrographs of worn surfaces were used to study the materials removal mechanisms of cold-sprayed Ni and Ni-WC coatings. Short and intermediate cycle's data were used to

11

evaluate the formation of tribolayers. Figure 6 shows the morphology of the wear track for Ni and Ni-WC coatings after 10 cycles. Significant plastic flow and adhesive wear, as evidenced by tongue-shaped structures and removal of patches of material (Fig. 6 indicated by white arrows), were observed for both coatings. This was consistent with the initial spike in CoF and wear rate at the beginning of the test. Extensive scoring of the surface in the sliding direction was observed on Ni coating worn surface (see Fig. 6c black arrows) as an indication of plowing wear that were not observed in the Ni-WC coating. Load bearing effect of relatively uniformly distributed WC particles in Ni-WC composite coating improved resistance to plastic deformation. As can be seen in Fig. 6b, Ni was preferentially worn away and squeezed up against WC particles. This led to earlier formation of tribolayers (see Fig. 6a black arrows) compared to the Ni coating.

As the tests progressed to further sliding cycles, the formation of MMLs became more evident (Figure 7). Detached particles within the wear track underwent repeated plastic deformation and oxidation. Wear particles with promoted work-hardening and oxidation were comminuted to fine size fragments. Because of adhesion forces existing between small size debris due to surface energy, fine debris were agglomerated at some regions and formed compact layers [19-21, 34]. For the Ni-WC coating, fragmentation of wear debris and formation of relatively compact layer was observed as early as 10 cycles (see Fig. 6a, black arrows). For the Ni coating, comminution of wear debris started later as observed for wear track morphology after 50 and 100 cycles (see Fig. 7c and d). However, the compactness of MML for the Ni coating was clearly less than that of the composite coating after 50 and 100 cycles (Fig. 7 a and b). Compact MML, in the case of Ni coating, formed at longer cycles (Fig. 7d,), but its coverage on the worn surface was lower than that of the composite coating. Likewise, 150-200 sliding cycles were needed for the Ni coating to reach steady-state COF value. However, loose wear debris on the

worn surface of the Ni coating acted as obstacles against the sliding and led to fluctuation in CoF for the Ni coating after reaching an initial steady state.

The wear track of the Ni-WC composite coating after 1000 cycles consisted of three main features, the elevated compact MML rich in oxygen (see Fig. 8a and c, black arrows), and low oxygen content zone in which Ni and oxygen intensity remaining roughly the same as unworn coating from the results of EDX (see Fig. 8a and c, white arrows) and wear debris, which covered the wear track. Part of the wear debris was ejected outside the wear track. Cracks on MML were also visible at higher magnification. The wear track of the Ni coating displayed similar morphology, but with less coverage of the MML and less wear debris compared to that of the Ni-WC coating. Abrasive grooves were observed in the Ni coating worn surface using higher magnification view of tribolayers (see Fig. 6d, white arrows). With adding WC into Ni, the worn surface was covered with MML to a larger extent and the amount of wear debris was significantly reduced.

Greater contrast between the Ni and WC was achieved from backscattered electrons (BSE) imaging in Fig. 9, representing worn surfaces of the Ni-WC composite coating at 10 and 1000 cycles. As can be seen, there was no pulled out WC detected on the worn surfaces, indicative of good cohesion between the Ni matrix and the WC particles [35]. However, surfaces were covered by fine fragmented WC particles, which were pulled out during sliding and redistributed on the surfaces as early as 10 cycles. These fine particles were retained between the two contacting surfaces and directly incorporated in the fast development of the compact layers. As demonstrated by worn surface features of the Ni-WC coating at 10 cycles (see Fig. 7c, black arrows), some regions of the wear track showed an early stage of MML development evidenced by the smoother surface compared to the smeared and layered structure around it. The fine redistributed WC particles not only facilitated fast development of the tribolayer, but also

improved its stability and increased hardness and contributed to superior sliding wear resistance of the Ni-WC coating compared to the Ni coating.

Significant improvement in sliding wear resistance with only small concentration of WC in Ni matrix was also reported in a previous study on laser cladded Ni-WC with 10 vol% WC tested at similar wear conditions [4]. The reported wear rate of 10×10^{-6} mm^3/Nm [4] is in good agreement with that of the present study. Adhesion and oxidation were reported to be dominant wear mechanisms for laser cladded Ni and Ni-WC coatings with WC concentrations lower than 25-30 vol% [3,7]. Although, adhesive wear was found to remain more pronounced for Ni coating, which is consistent with this study [3].

A transition to three-body abrasive wear was found at higher WC concentrations, where WC particles can be easily dislodged from surface and trapped in contact due to cracking at interfaces [3,7]. These cracks are originated from brittle phases at interface and also significant residual stress at higher concentration of WC in coating [3,4]. However, these defects can be avoided using cold spray. While previous findings shows that a significant decrease in wear does not occur above approximately 25-30 vol% WC in laser cladded composite coatings, retention of high content WC to cold sprayed coating is challenging. Although higher WC concentration wasn't achieved in this study using cold spray at applied conditions, testing of processing parameters and initial feedstock are currently in progress to improve the efficiency of the process.

Figure 10 shows morphology of the wear debris outside the wear tracks for Ni and Ni-WC composite coatings. In the Ni-WC worn surface, compacted fine wear debris of 1 - 5 µm in size was observed, while plate-like wear debris up to 100 µm in size was found in the Ni coating. The scale of the wear debris also correlated to tribological behavior, where the Ni coating, with larger wear debris, exhibited a higher wear rate than the Ni-WC coating, with smaller wear debris.

During initial contact of the WC-Co ball on the coatings surface, high contact stress is expected to occur. The initial Hertzian contact stress [36,37] for Ni and Ni-WC coatings were estimated to be 718-723 MPa and 794-805 MPa, respectively. The predicted contact stress is only valid during initial contact of two mating surfaces. As sliding progresses, plastic deformation, materials transfer, wear debris generation and etc occur, contact stresses become far more complicated. In the present study, both coatings caused wear of counterparts and contributed to a drop in contact pressure. The morphologies of worn surface of the WC-Co ball after 1000 cycles sliding against Ni and Ni-WC coatings are shown in Fig.11. The apparent contact stresses after 1000 cycles sliding for Ni and Ni-WC coatings were estimated to be 36 and 41 MPa, respectively. WC–Co ball mating with Ni coating underwent more severe wear under lower contact stress, which may come from the bigger wear debris generated during the wear process, as plate-like debris can be also observed (Fig. 11b indicated by arrow).

3.3.2. Subsurface microstructure

Figure 12 shows BSE micrographs of wear track cross sections taken perpendicular to the sliding direction for Ni and Ni-WC composite coatings at 1000 cycles. In both cases, a layer of mixed material with a thickness of about 5 μm was found at the surface. The layer consisted of Ni fragments detached from surfaces and nano-crystalline Ni rich in oxygen, covered the top of worn surfaces. For cross-section of the wear track of the Ni coating (Fig. 12a), subsurface micro-cracking was observed. This was attributed to the shear stresses transferred to the bulk surface material underneath the MML due to low load bearing capacity of Ni which resulted in a larger tendency for plastic deformation of asperity junctions [38]. The intersection of these cracks led to detachment of wear particles. The hard particles detached from MML acted as third-bodies abrasive particles which induced wear on sliding surfaces and resulted in increased wear rate and made CoF fluctuate. However, in the case of the Ni-WC composite coating, the development of a

coherent and stable MML, which is evident from Fig. 12b, contributed to superior wear resistance of the Ni-WC coating compared to the Ni coating. The presence of fine redistributed WC particles in the MML improved friction stability as evidenced by stable CoF.

3.3.4. Hardness and elemental composition of third bodies

The hardness of the MML of cold-sprayed Ni and Ni-WC composite coatings were measured using nano-indentation. In the unworn Ni and Ni-WC coatings, the average hardness of the pure Ni was 4.6 ± 1.0 and 5.2 ± 1.0 GPa, respectively, which showed significant increase in hardness value compared to that of the Ni feedstock powder (2.1 ± 0.2 GPa). This is due to extensive plastic deformation, grain refinement, and increased local dislocation density [10]. The MML of the Ni coating had a hardness of 6.2 ± 0.7 GPa which was 1.4 times higher than that of the underlying Ni. This is similar to the degree of hardening in the tribolayer of micro and nano-crystalline Ni subjected to dry wear sliding test, which was 1.3-1.5 times, reported in a previous study [39]. The strain hardening due to grain refinement and surface oxidation are the possible contributions to the increased hardness of MML [39]. The hardness of the Ni-WC coating's MML was 11.2 ± 3.6 GPa which was 2.2 times harder than the bulk of the tested material. Several previous studies have reported increases in MML's hardness for metal matrix composites compared to the underlying materials. A large value of hardness of the worn surface was due to the redistributed fine WC particles and strain hardening.

Elemental microanalysis of the unworn and the wear tracks of coatings revealed increased oxygen in the worn surfaces. Representative EDX spectra were collected from the regions of interests. In the EDX spectra, the relative intensities of Kα peaks of oxygen and Ni are centered at 0.53 and 0.85 keV, respectively. In the unworn Ni, the Ni peak was dominant with a small oxygen peak; whereas in the Ni coating's MML, the Ni peak intensity remained roughly the same as the unworn coating, but oxygen peak intensity increased. The Ni-WC coating MML showed

16

roughly equal intensity of Ni, however, a larger presence of oxygen was measured. There are several possible reasons for increased oxygen content in the worn surfaces. One is materials mixing during sliding where clean metal is exposed to oxygen [40]. This can be promoted by deformation heat and an increased energy level of particles due to sliding induced defects and surface energy [19,20]. The higher oxygen content in the load-bearing areas of Ni-WC composite coating and fine debris around these areas compared to those of the Ni coating can be attributed to more localized plastic deformation of MML due to its higher hardness.

4. Conclusion

Using the cold spray process, Ni and Ni-WC coatings were deposited and their tribological behavior during dry sliding wear was studied and compared. Inclusion of WC resulted in a reduction in coating porosity. However, the presence of WC particles decreased deposition efficiency and also reduced bonding between Ni particles. Much less WC particles were retained (10.5 vol%) than in feedstock (36.2 vol%). For the sliding wear, the presence of WC particles in the coating stabilized CoF and decreased wear rate by a factor of seven. This improvement was linked to the formation of a stable and cohesive MML on top of the wear track of Ni-WC coating which protected first bodies from wear. This, in turn, was attributed to the fine fragmented WC particles which were redistributed during sliding and enhanced resistance to plastic flow of Ni matrix. Fine fragmented WC particles facilitated the fast development of MML, as well as, improved its stability and increased its hardness which contributed to superior wear resistance of composite.

References

[1] J. R. Davis, *Handbook of thermal spray technology,* ASM international, 2004 .

[2] Y.P. Kathuria, Some aspects of laser surface cladding in the turbine industry, Surf. Coat. Technol. **132** (2000) 262-269.

[3] M.R. Fernández, A. García, J.M. Cuetos, R. González, A.Noriega, M.Cadenas, Effect of actual WC content on the reciprocating wear of a laser cladding NiCrBSi alloy reinforced with WC, Wear. **324-325** (2015) 80-89.

[4] K. Van Acker, D. Vanhoyweghen, R. Persoons, J. Vangrunderbeek, Influence of tungsten carbide particle size and distribution on the wear resistance of laser clad WC/Ni coatings, Wear. **258** (2005) 194–202.

[5] P. Wu, H.M. Du, X.L. Chen, Z.Q. Li, H.L. Bai, E.Y. Jiang, Influence of WC particle behavior on the wear resistance properties of Ni–WC composite coatings, Wear. **257** (2004) 142–147.

[6] C. Guo, J. Zhou, J. Chen, J. Zhao, Y. Yua, H. Zhou, High temperature wear resistance of laser cladding NiCrBSi and NiCrBSi/WC-Ni composite coatings, Wear. 270 (2011) 492–498.

[7] J.S. Xu, X.C. Zhang, F.Z. Xuan, Z.D. Wang, and S.T. Tu, Microstructure and sliding wear resistance of laser cladded WC/Ni composite coatings with different contents of WC particle, J Mater Eng Perform. 21(9) (2012) 1904–1911.

[8] V.K. Champagne, *The cold spray materials deposition process fundamentals*,Woodhead Publishing, 2007.

[9] A. Papyrin,V. Kosarev,S. Klinkov,A. Alkhimov, V. Fomin, *Cold spray technology*, Elsevier, 2006.

[10] Y. Zou, D. Goldbaum, J. A. Szpunar, S. Yue, Microstructure and nanohardness of cold-sprayed coatings: Electron backscattered diffraction and nanoindentation studies, Scripta Mater. **62** (2010) 395-398.

[11] F. Sevillano, P. Poza, C. J. Mu´nez, S. Vezzu`, S. Rech, and A. Trentin, Cold-Sprayed Ni-Al2O3 Coatings for Applications in Power Generation Industry, J. Therm. Spray Technol.22-5 (2013) 772–782.

[12] J. Wang, J. Villafuerte, *Processing and properties of advanced ceramics and composite, Wiley, 2009.*

[13] C. J. Li, G. J. Yang, P.H. Gao, J. Ma, Y. Y. Wang, C.-X. Li, Characterization of nanostructured WC-co deposited by cold spraying, J. Therm. Spray Technol. **16** (2007) 1011-1020.

[14] R. Lima, J. Karthikeyan, C. M. Kay, J. Lindemann, C. C. Berndt, Microstructural characteristics of cold-sprayed nanostructured WC–Co coatings, Thin Solid Films. **416** (2002) 129-135.

[15] P. H. Gao, Y. G. Li, C. J. Li, G. J. Yang, and C. X. Li, Influence of powder porous structure on the deposition behavior of cold-sprayed WC-12Co coatings, J. Therm. Spray Technol. **17** (2008) 742-749.

[16] M. Couto, S. Dosta, M. Torrell, J. Fernández, J.M. Guilemany, Cold spray deposition of WC–17 and 12Co cermets onto aluminum, Surf. Coatings Technol. **235** (2013) 54-61.

[17] H. J. Kim, C. H. Lee, S.Y. Hwang, Fabrication of WC–Co coatings by cold spray deposition, Surf. Coatings Technol. **191** (2005) 335-340.

[18] M. Godet, The third-body approach: A mechanical view of wear, Wear. **100 1-3** (1984) 437-452.

[19] J. Jiang, F. H. Stott and M. M. Stack, The role of triboparticulates in dry sliding wear, Tribology International. **31** (1998) 245-256.

[20] J. Jiang, F.H. Stott, M.M. Stack, Some frictional features associated with the sliding wear of the nickel-base alloy N80A at temperatures to 250 °C, Wear. **176** (1994) 185-194.

[21] B. Venkataraman, G. Sundararajan, Correlation between the characteristics of the mechanically mixed layer and wear behaviour of aluminium, Al-7075 alloy and Al-MMCs, Wear. **245** (2000) 22-38.

[22] R. Gonz´alez, M. Cadenas, R. Fern´andez, J.L. Cortizo, E. Rodr´ıguez, Wear behaviour of flame sprayed NiCrBSi coating remelted by flame or by laser, Wear. **262** (2007) 301-307.

[23] J.M. Shockley, H.W. Strauss, R.R. Chromik, N. Brodusch, R. Gauvin, E. Irissou, J.-G. Legoux, In situ tribometry of cold-sprayed Al-Al2O3 composite coatings, Surf. Coat. Technol. **215** (2013) 350-356.

[24] W. C. Oliver and G. M. Pharr, An improved technique for determining hardness and elastic modulus using load and displacement sensing indentation experiments, J. Mater. Research. **7-6** (1992) 1564-1583.

[25] B. Bhushan, Principles and applications of tribology, Wiley, 2006.

[26] T. Schmidt, F. Gärtner, H. Assadi, H. Kreye, Development of a generalized parameter window for cold spray deposition, Acta Mater. **54** (2006) 729-742.

[27] R.C. Dykhuizen, M.F. Smith, Gas dynamic principles of cold spray, J. Therm. Spray Technol. **7** (1998) 205-212.

[28] H. Koivuluoto, P. Vuoristo, Effect of ceramic particles on properties of cold-sprayed Ni-20Cr+Al2O3 coatings, J. Therm. Spray Technol. **18-4** (2009) 555–562.

[29] V.K. Champagne, The repair of magnesium rotorcraft components by cold spray, J. Fail. Anal. Prev. **8** (2008) 164-175.

[30] D. Helfritch, O. Stier and J. Villafuerte, Cold Spray Economics, in: J. Villafuerte, Modern Cold Spray: Materials, Process, and Applications, Cham: Springer, 2015, pp. 377-401.

[31] X.T. Luo, C. J. Li, Large sized cubic BN reinforced nanocomposite with improved abrasive wear resistance deposited by cold spray, Mater. & Des. **83** (2015) 249-256.

[32] P.C. King, S.H. Zahiri, M. Z. Jahedi, Rare earth/metal composite formation by cold spray, J. Therm. Spray Technol. **17-2** (2007) 221-227.

[33] R.B. Waterhouse, The role of adhesion and delamination in the fretting wear of metallic materials, Wear **45** (1977) 355-364.

[34] K. Triantou, D.Pantelis, V. Guipont, M. Jeandin, Microstructure and tribological behavior of copper and composite copper+alumina cold sprayed coatings for various alumina contents, Wear **336-337** (2015) 96-107.

[35] N. Kang, P. Coddet, H. Liao, C. Coddet, The effect of heat treatment on microstructure and tensile properties of cold spray Zr base metal glass/Cu composite, Surf. Coat. Technol. **280** (2015) 64-71.

[36] K.L. Johnson, Contact Mechanics. Cambridge University Press, Cambridge, 1985.

[37] T.W. Clyne, P.J. Withers, An introduction to metal matrix composites, Cambridge University Press, Cambridge, 1995.

[38] Z. Guo-gang, Z. Yue-bo, Z. Hai-jun, Sliding wear behaviors of electrodeposited Ni composite coatings containing micrometer and nanometer Cr particles, Trans. Nonferrous Met. Soc. China. **19** (2009) 319-323.

[39] M. Shafiei, A. Alpas, Friction and wear mechanisms of nanocrystalline nickel in ambient and inert atmospheres, Metal. Mat. Transac. **38A** (2007) 1621-1631.

[40] J.R. Davis, *Corrosion Behavior*, ASM International, Materials Park, Ohio, 1993.

Figures Captions

Figure 1 – Morphology and size distribution of the as-received powders: (a) and (b) Ni, (c) and (d) WC powder.

Figure 2 – Cross-section morphology (a) and top-down morphology (b) of the Ni coating, (c) high magnification view of (b).

Figure 3 – Cross-section morphology (a) and top-down morphology (c),(d) of the Ni-10.5vol% WC coatings, (b) and (e) high magnification view of (a) and (d), respectively. Black arrows indicate adhered WC particles to surface. White arrows indicate WC fragments.

Figure 4 – Average friction coefficient plotted versus number of cycles for tests run to 1000 cycles on cold sprayed Ni and Ni-10.5 vol%WC coatings.

Figure 5 – Volumetric wear rate plotted versus number of cycles.

Figure 6 – Morphology of (a) Ni-10.5vol%WC, where black arrows indicate early formation of tribolayers and (c) Ni wear track after 10 sliding cycles, where black arrows indicate scoring of surface (b) and (d) high magnification view of (a) and (c), respectively. White arrows indicate tongue-shaped features.

Figure 7 – Morphology of (a), (b) Ni-10.5vol%WC and (c), (d) Ni wear track after (a),(c) 50 and (b),(d) 100 sliding cycles. Black arrows indicate tribolayers.

Figure 8 – Morphology of (a) Ni-10.5vol%WC and (c) Ni wear track after 1000 sliding cycles, (b) and (d) high magnification view of (a) and (c), respectively. Black arrows indicate tribolayers. White arrows indicate abrasive grooves and cracks.

Figure 9 – Backscattered image of cross-section of Ni-10.5vol%WC coatings after (a) 10 and (c) 1000 sliding cycles, (b) and (d) high magnification view of (a) and (c), respectively.

Figure 10 – Morphology of wear debris outside the wear track of (a) Ni-10.5vol%WC and (b) Ni coatings.

Figure 11 – Morphology of the worn surfaces of the WC-Co ball mating with the (a) Ni-10.5vol%WC and (b) Ni coatings. Black arrow indicates plate-like debris.

Figure 12 – Cross-sections of the near-surface microstructures after 1000 sliding cycles for (a) Ni, where black arrows indicate Ni fragments and white arrows indicate oxygen rich regions, and (b) Ni-10.5vol%WC coatings, where black arrows indicate WC fragments and white arrows indicate oxygen rich regions. SD indicates sliding direction.
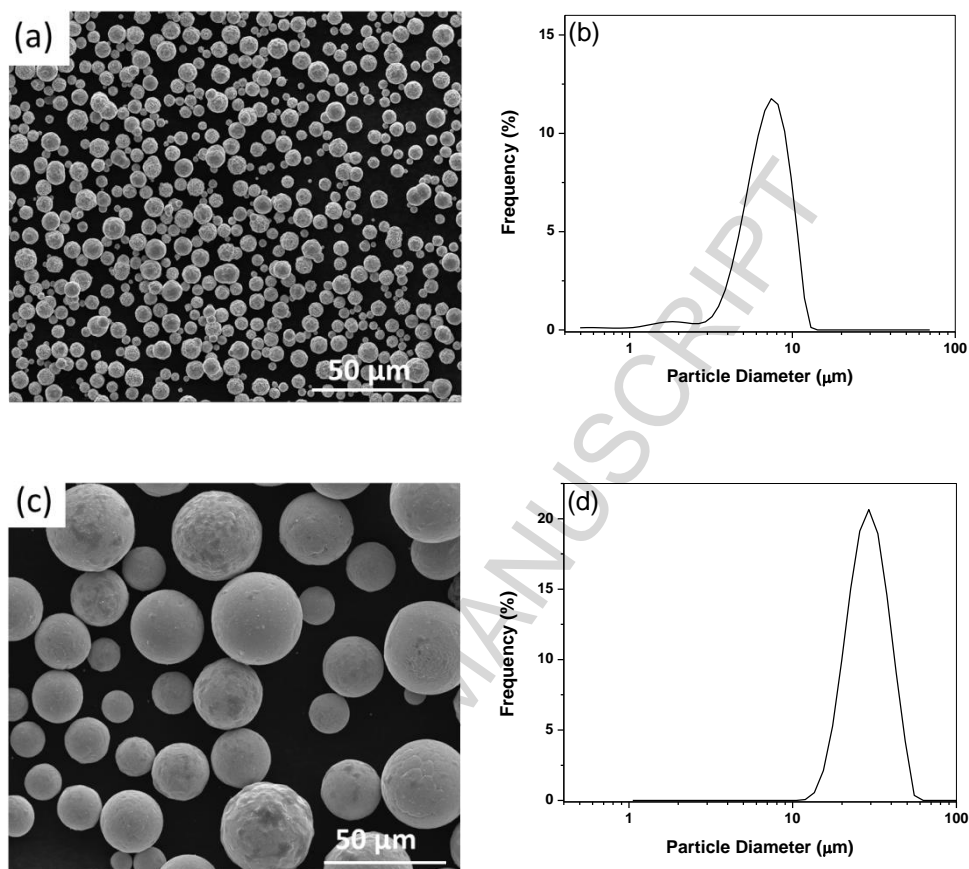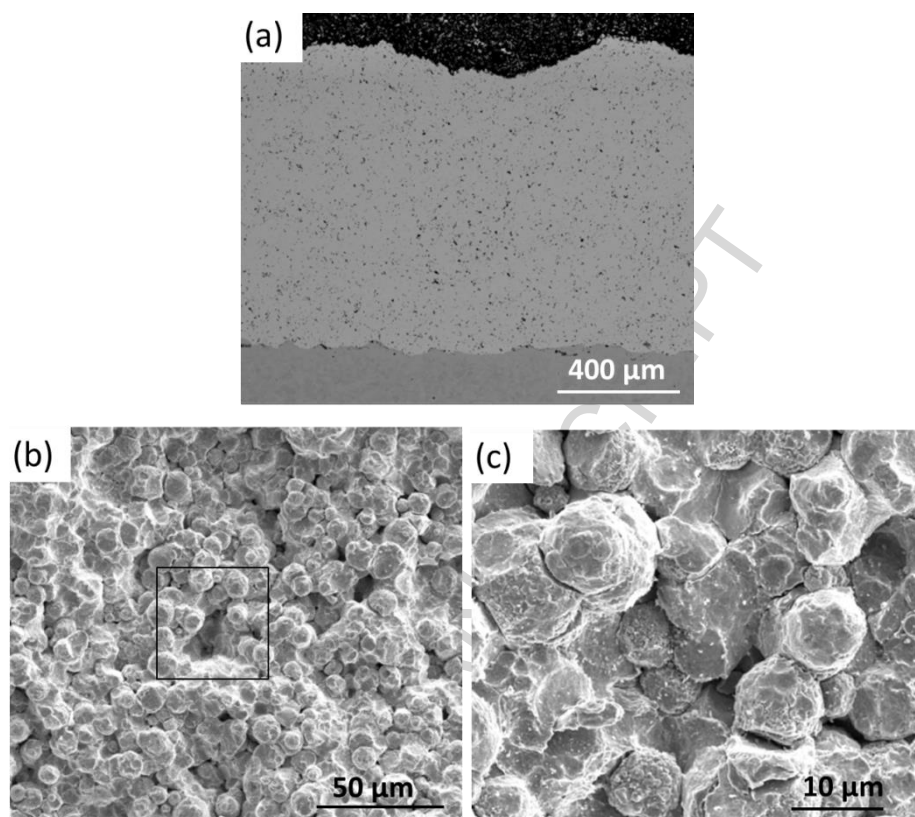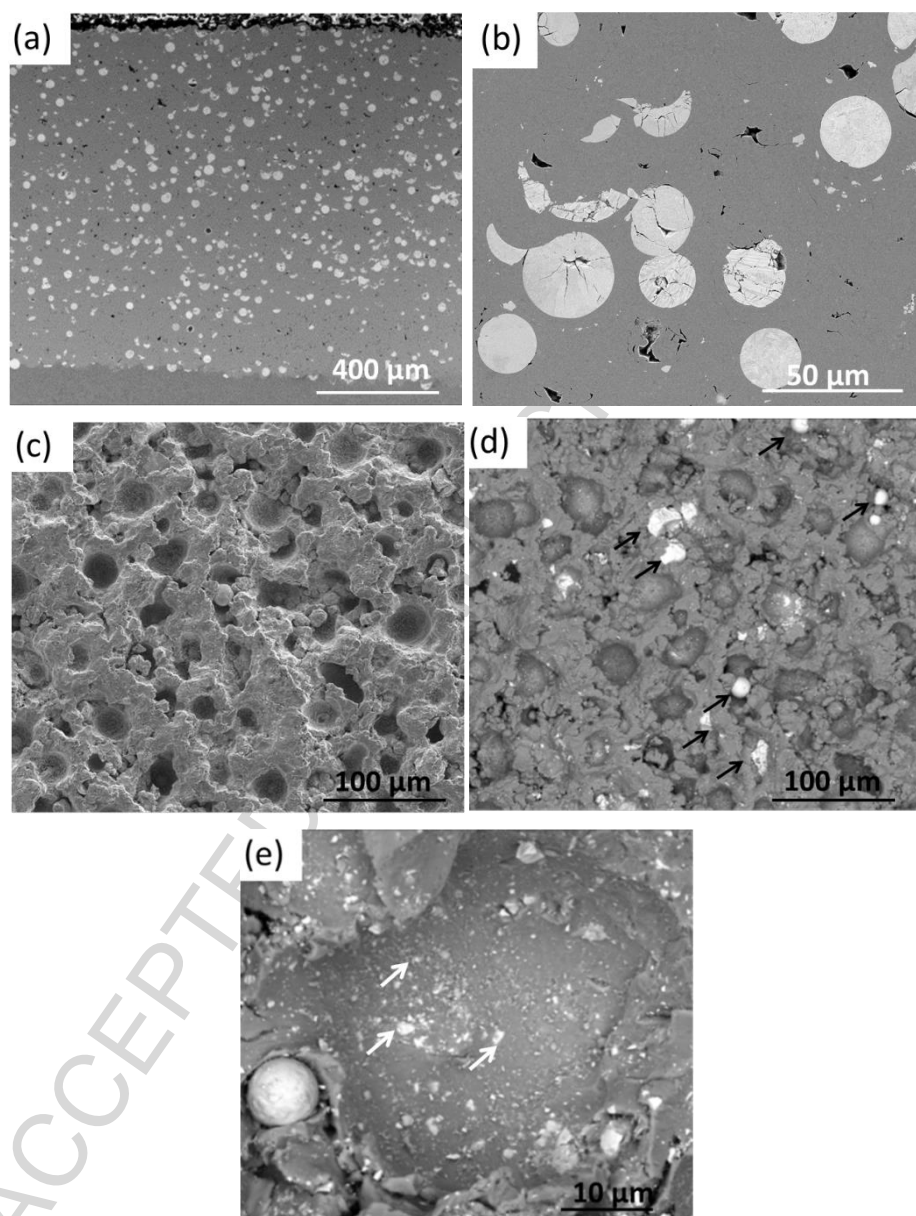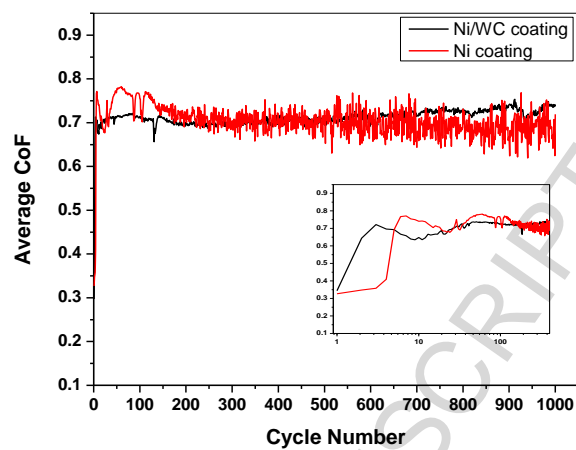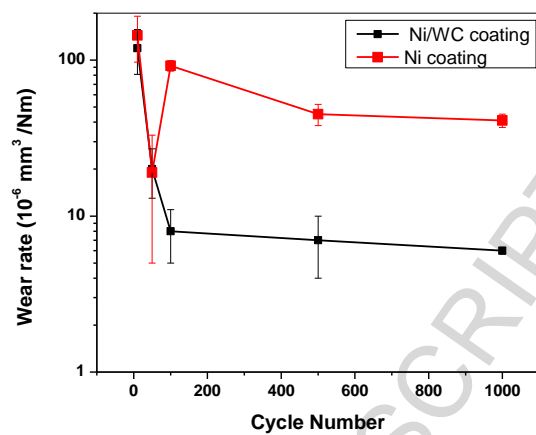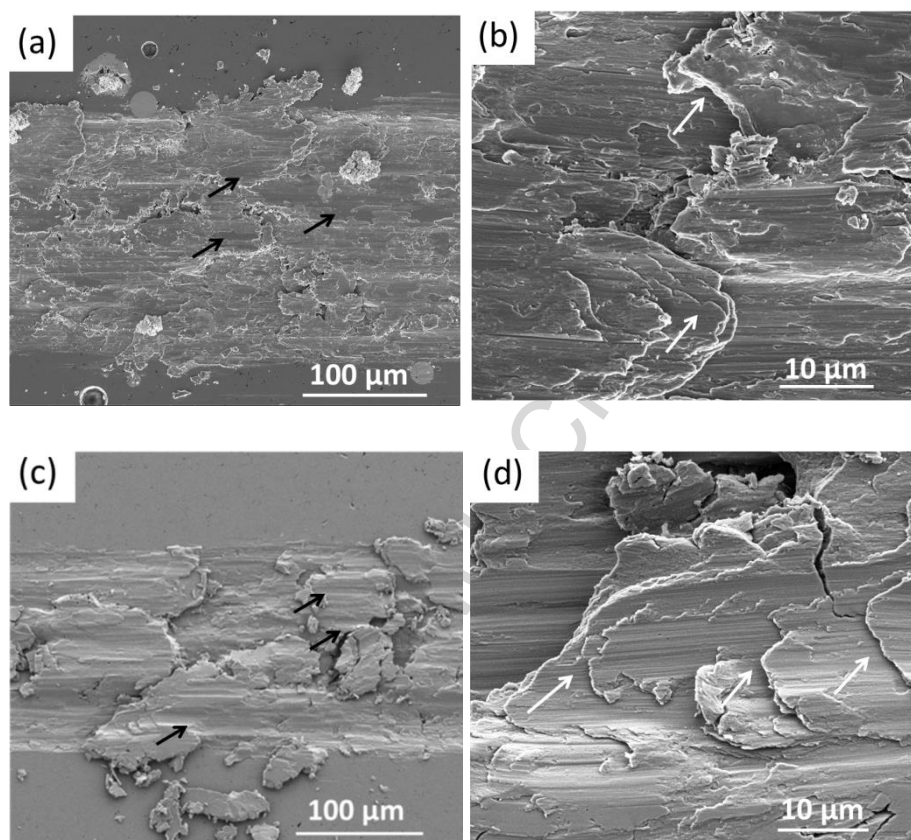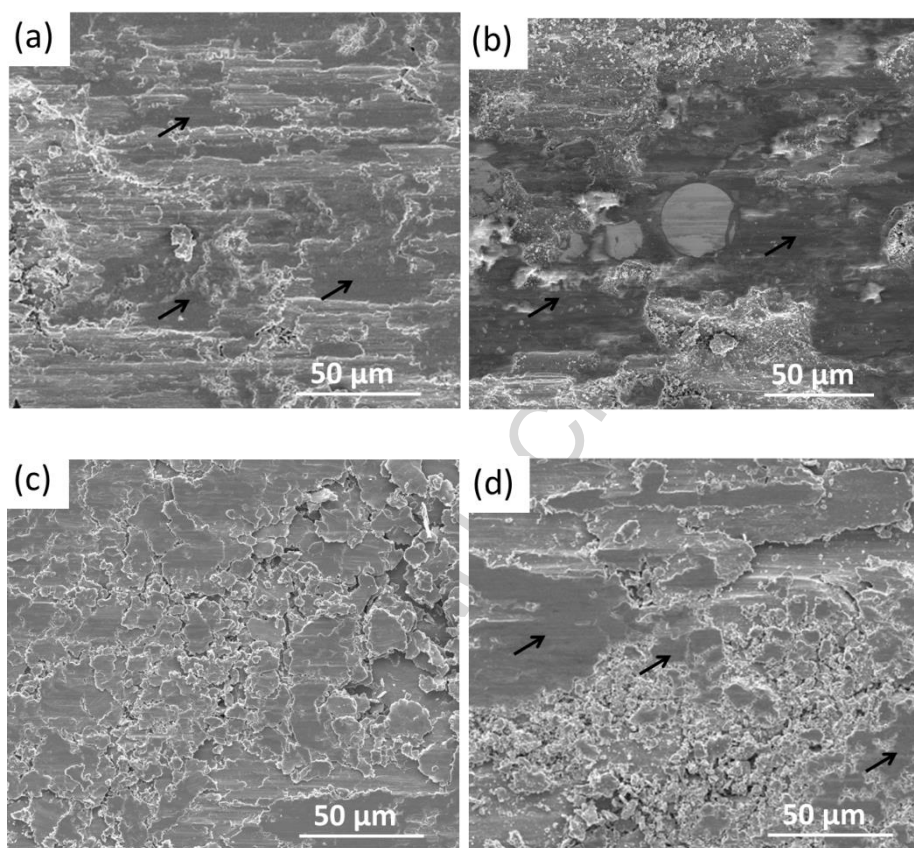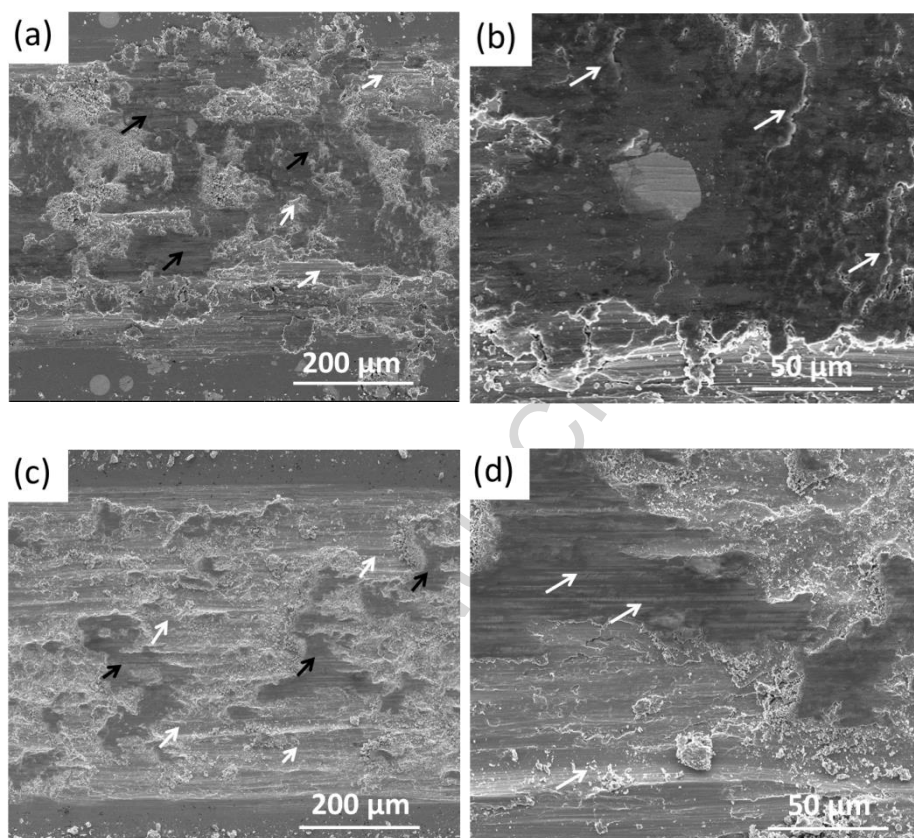
Figure 1

Figure 2

Figure 3

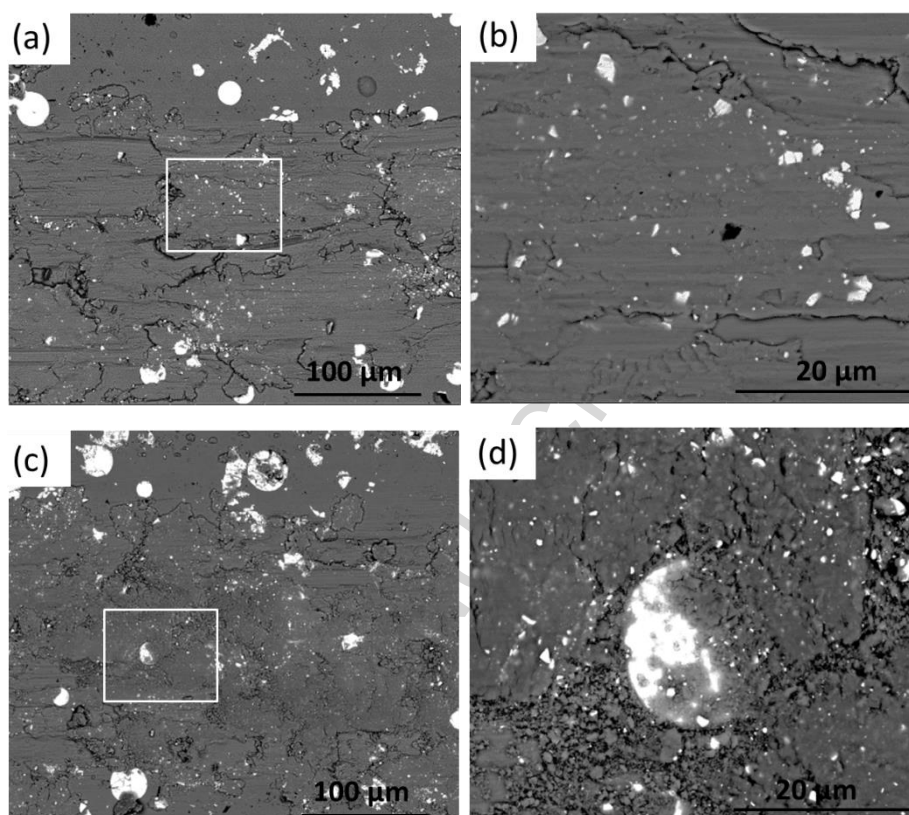Figure 4

Figure 5

Figure 6

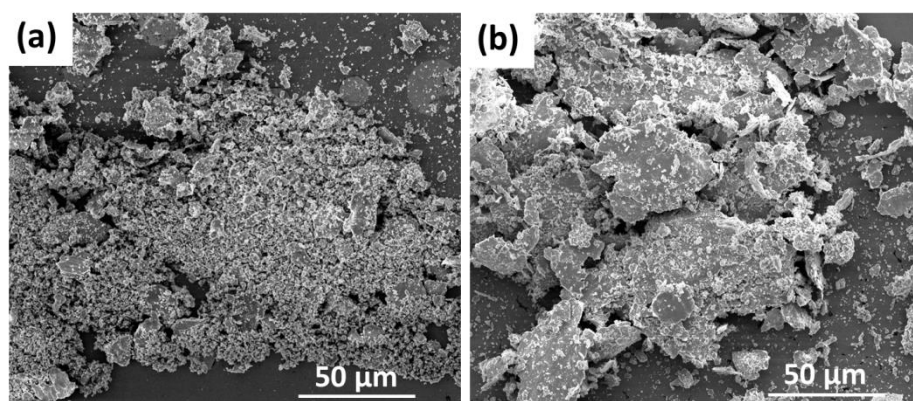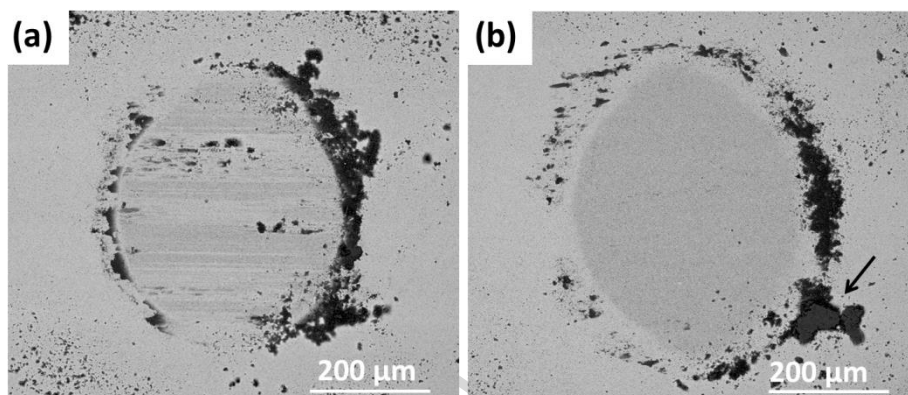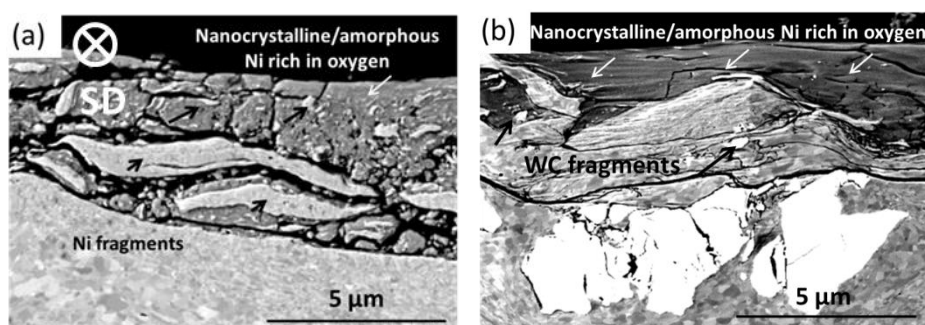Figure 7

Figure 8

Figure 9

Figure 10

Figure 11

Figure 12

Highlights:

- Presence of tungsten carbide (WC) decreased deposition efficiency of Nickel.
- WC particles were mainly entrapped to coating by later-arriving particles.
- Incorporation of WC into Nickel improved its sliding wear resistance significantly.
- Improvement was due to fast development of the harder and more stable tribolayer.